

# Temkin-Pyzhev Kinetics in Intermediate Temperature Ammonia-Fed Solid Oxide Fuel Cells (SOFCs)

Denver F. Cheddie

Mechanical Engineering, University of Trinidad and Tobago, Point Lisas Campus, Esperanza Road, Brechin Castle, Couva, Trinidad and Tobago  
Email: denver.cheddie@utt.edu.tt

**Abstract.** Two recent trends in fuel cell development are the use of ammonia as a fuel, and the preference for intermediate temperature operation of solid oxide fuel cells. There have been a few mathematical models of ammonia-fed solid oxide fuel cells reported in the literature, all of which are for high temperature operation where Tamaru kinetics applies. To date, there have been no models reported for intermediate temperature operation. At intermediate temperatures, hydrogen inhibition of ammonia decomposition occurs and hence the Temkin-Pyzhev model of ammonia decomposition must be employed. This paper is the first to present a two-dimensional computational model of an intermediate temperature ammonia-fed solid oxide fuel cell with Temkin-Pyzhev ammonia decomposition kinetics. The results show that the problem of thermal shock associated with high temperature ammonia-fed fuel cells is alleviated at intermediate temperature operation.

**Keywords:** Ammonia, solid oxide fuel cells, intermediate temperature, Tamaru kinetics, Temkin-Pyzhev model.

## 1 Introduction

### 1.1 Ammonia as a Fuel for Solid Oxide Fuel Cells

The high operating temperature of solid oxide fuel cells (SOFCs) allows for a wide variety of fuels including hydrogen, methane, natural gas, methanol, ethanol and carbon dioxide. These fuels pose problems for wide scale usage. Hydrogen is difficult to store and transport, while the others are all carbon based.

Recently, ammonia has been considered as a fuel for SOFCs. It possesses a higher volumetric energy density than pure hydrogen, compressed natural gas, and methanol [1]. It is widely produced and distributed globally [2]. It produces zero carbon emissions and negligible nitrogen oxide (NOx) emissions [3-6]. Cheddie [7] provides a comprehensive review on the use of ammonia as a hydrogen source for fuel cells.

Because of the high temperature of SOFC operation, ammonia is decomposed into nitrogen and hydrogen using thermal energy present within the fuel cell anode, as shown in equation 1. Thus ammonia serves as a hydrogen source. It is thermodynamically possible to achieve 98-99% conversion of ammonia at temperatures as low as 425 °C [8], however the reaction kinetics are slow. Catalysts such as Pt, Ru, Pd, and Ir are required to speed up the rate of decomposition [9-12].



Promising results have been demonstrated with a Ru catalyst, which provides nearly complete conversion of ammonia to hydrogen at 600 °C, 64% conversion at 500 °C, and 14% at 400 °C [9]. However, the high cost of Ru militates against mass production for fuel cell applications. A lower cost alternative is Ni [9, 13-17], which has resulted in 70% conversion of ammonia at 650 °C [9], 72% conversion at 500 °C [16] and 95% conversion at 600 °C [13].

## 1.2 Intermediate Temperature Operation of SOFCs

There is also a trend in SOFC research to reduce the temperature of operation. High temperature SOFCs (800 – 1000 °C) require expensive ceramic electrolyte materials such as yttria stabilized zirconia (YSZ) and samaria-doped ceria (SDC). These are oxygen ion conducting electrolytes which require high temperatures to maintain high ionic conductivity. The high temperature environment also results in rapid degradation of the materials.

The discovery of proton conducting electrolytes, such as barium cerate, has allowed for a reduction in SOFC operating temperature without compromising electrolyte conductivity [7]. Barium cerate electrolytes have been successfully implemented in SOFCs operating at 600-700 °C, and in one report, an SOFC based on a barium cerate electrolyte was successfully operated at 450 °C [18]. These intermediate temperatures are preferable from a materials point of view. The challenge for intermediate temperature ammonia-fed SOFCs is maintaining a high conversion of ammonia to hydrogen at the lower temperatures.

Early works found that when 1) the operating temperature was below 400 °C, 2) the ammonia partial pressure was low, and 3) the hydrogen partial pressure was high; the hydrogen which was produced in the decomposition reaction inhibited the rate of ammonia decomposition [19]. This phenomenon is called hydrogen inhibition. The Tamaru kinetic model of ammonia decomposition is appropriate for cases where hydrogen inhibition does not occur, while the Temkin-Pyzhev model is appropriate when hydrogen inhibition does occur [20].

Based on experimental data, Chellappa et al [19] concluded that hydrogen inhibition does not occur at temperatures above 400 °C. However, it is noteworthy that they arrived at that conclusion based on experimental data conducted between 520-660 °C. They noted that their data was accurately fitted to the Tamaru model, and hence they concluded that Temkin-Pyzhev kinetics do not apply. However, Vilekar et al [21] have shown that the same experimental data of Chellappa et al [19] could also be accurately fitted to the Temkin-Pyzhev model. They concluded that the Temkin-Pyzhev model is valid for operating temperatures up to 660 °C. Other works have confirmed that the Temkin-Pyzhev model could accurately fit experimental data up to 600 °C [22-24]. This shows that hydrogen inhibition is likely to occur up to at least 660 °C, and as such it is a relevant concern for intermediate temperature SOFCs.

This casts aspersions on the conclusions drawn by Chellappa et al [19]. Logically it is unlikely that there would be a single temperature demarcating whether or not hydrogen inhibition occurs. More than likely, there would be a range of temperatures where both the Tamaru and Temkin-Pyzhev kinetic models would apply. Based on the experimental data, this temperature range would be 520-660 °C. Above this range, we can conclude that hydrogen inhibition does not occur and the Tamaru kinetic model is applicable for ammonia decomposition. Below this range, hydrogen inhibition is significant, and hence the Temkin-Pyzhev model is appropriate. But within this temperature range, both models could be used accurately.

## 1.3 Modeling of Ammonia-Fed SOFCs

Modelling of ammonia-fed SOFCs has not received a lot of attention in the literature since it is a recent trend. Most of the models presented to date are based on high temperature (700 – 800 °C) oxygen ion conducting SOFCs [25-33]. As a result, they do not consider the effects of hydrogen inhibition.

The first models of ammonia-fed SOFCs were thermodynamic (zero-dimensional) models which included first and second law analyses [25,26,31]. Ni et al [28,30] later developed electrochemical models to account for electrode kinetics. In another work, they incorporated their electrochemical models with their previous thermodynamic model to further develop the state of the art in ammonia-fed SOFC modelling [32]. They presented this model for both oxygen ion conducting electrolytes as well as proton conducting electrolytes, however, all of the modelling was conducted at high temperatures [29]. Cheddie [33] continued the development of the field by presenting a computational fluid dynamics model.

The most significant finding in these works is that because of the endothermic ammonia decomposition reaction occurring in the SOFC anode, there was a significant temperature drop followed by a temperature increase due to the exothermic fuel cell reactions. This resulted in a temperature sink or cold spot within the SOFC anode. Ni et al [32] reported this temperature drop to be 67 °C which would pose deleterious material degradation problems in the SOFC anode. Cheddie [33] investigated

strategies to reduce this temperature drop. It was found that recycling some of the anode outlet back into the inlet feed served to reduce the inlet ammonia partial pressure, and hence reduce the rate of decomposition. This strategy reduced the temperature sink to 24 °C.

Essentially, the best strategies to alleviate the temperature sink involve reducing the rate of ammonia decomposition. Naturally if the operating temperature is decreased, the rate of ammonia decomposition will also decrease, thus intermediate temperature operation is likely to solve the temperature sink problem reported in the literature.

All of the reported models were applied to high temperature SOFCs and thus incorporated Tamaru kinetics. None of these works attempted to model intermediate temperature SOFCs where hydrogen inhibition occurs. To date, there have been no reported models of intermediate temperature ammonia-fed SOFCs accounting for hydrogen inhibition.

## 1.4 Objective

This paper is the first model to report a two-dimensional computational model of an intermediate temperature ammonia-fed SOFC which considers the effects of hydrogen inhibition and incorporates Temkin-Pyzhev kinetics. It builds on our previously published model of an ammonia reactor employing Temkin-Pyzhev kinetics [33]. This paper applies the model to an entire solid oxide fuel cell.

## 2 Model Development

### 2.1 Computational Domain

The computational domain shown in Figure 1 is for a 2D planar SOFC, however, the model can easily be applied to tubular SOFC geometry.

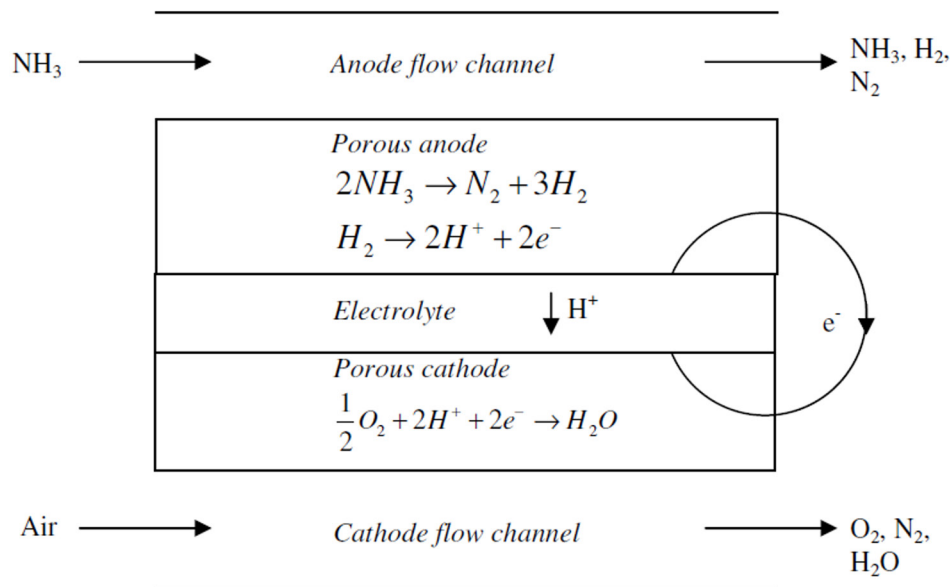


Figure 1. Computational Domain.

Pure ammonia is supplied to the anode while atmospheric air enters the cathode. In this model, ammonia decomposes into hydrogen and nitrogen in the anode porous domain in accordance with Temkin-Pyzhev kinetics. The rate of decomposition is given by [22],

$$r_{NH_3} = (6 \times 10^7) \exp\left(-\frac{95600}{RT}\right) \left(\frac{p_{NH_3}^2}{p_{H_2}^3}\right)^{0.209} \quad (2)$$

Hydrogen then reacts electrochemically at the anode / electrolyte interface.



## 2.2 Governing Differential Equations

In the present model, the Navier-Stokes equations with Darcy's Law source term are used to model bulk fluid flow. The heat equation is used to determine the temperature distribution. Chemical species transport is modelled using the dusty gas model, which is considered the most accurate model for chemical species transport in porous media since it accounts for Knudsen diffusion [35]. The Butler-Volmer equation is used for the electrochemical half-cell reactions. These equations are listed below.

$$\rho u \cdot \nabla u = \nabla p + \nabla(\mu \nabla u) + \frac{\mu}{\beta} u \quad (5)$$

$$\nabla \cdot (\rho c_p u T) = \nabla(k \nabla T) + S_T \quad (6)$$

$$\frac{N_i}{D_{i,k}^{eff}} + \sum_{j \neq i} \frac{x_j N_i - x_i N_j}{D_{i,j}^{eff}} = -\frac{\nabla(x_i p)}{RT} \quad (7)$$

$$\nabla \cdot N_i = S_i \quad (8)$$

$$\nabla \cdot (\sigma_e \nabla \phi_e) = 0 \quad (9)$$

$$j = 2j_{0,a}^{ref} \frac{c_{H_2}}{c_{H_2}^{ref}} \frac{c_{H_2O}^{ref}}{c_{H_2O}} \sinh\left(\frac{F\eta_{act,a}}{RT}\right) \quad (10)$$

$$j = 2j_{0,c}^{ref} \left(\frac{c_{O_2}}{c_{O_2}^{ref}}\right)^{1/2} \sinh\left(\frac{F\eta_{act,c}}{RT}\right) \quad (11)$$

## 2.3 Source Terms

The heat generation source terms are both interfacial and volumetric. The electrochemical reactions are reckoned at the electrode / electrolyte interfaces, therefore reaction heat sources are interfacial. Ohmic heating is dominant in the electrolyte domain. The endothermic ammonia decomposition occurs in the anode, and represents a heat sink in the anode domain.

$$S_{H_2} = -j \frac{M_{H_2}}{2F} \quad (12)$$

$$S_{O_2} = -j \frac{M_{O_2}}{4F} \quad (13)$$

$$S_{H_2O} = +j \frac{M_{H_2O}}{2F} \quad (14)$$

$$S_{T,decomp} = -r_{NH_3} \Delta H_R \quad (15)$$

$$S_{T,fuelcell} = j \left( \eta - \frac{T\Delta s}{2F} \right) \quad (16)$$

## 2.4 Solver

The model is implemented in COMSOL MultiPhysics 4.3, with a mesh containing 18,500 rectangular elements, and is solved on a 2 GB, 2 GHz Intel CPU platform using the MUMPS direct stationary non-linear solver.

### 3 Results

All of the results shown in this section are based on an operating cell potential of 0.7 V, current density of 5000 A/m<sup>2</sup>, and inlet temperature of 500 °C (773 K) of supply gases. Figure 2 shows the ammonia mole fraction at the anode. Ammonia enters the anode channel at 1 atm. Within the anode domain, it decomposes into hydrogen and nitrogen and as a result its concentration decreases both in the direction of bulk flow and also in the direction anode-to-electrolyte. Note that the lowest mole fraction of ammonia is 0.83 indicating a low conversion rate.

Figure 3 shows the corresponding plot for hydrogen mole fraction. The inlet gas has zero hydrogen. But the hydrogen concentration increases as it is produced in the anode, but simultaneously decreases as it is consumed in the electrochemical reactions. At 0.7 V, the maximum hydrogen mole fraction is 0.0864. If there were no electrochemical reactions occurring at the anode/electrolyte interface, the maximum hydrogen mole fraction would have been higher.

Figure 4 shows the steady state temperature distribution. Cathode and anode gases enter at 773 K. For these conditions, the changes in temperature are not large. It decreases to a minimum value of 770.3 K and increases to a maximum of 774.2 K. This temperature sink is due to the endothermic ammonia decomposition reaction. The temperature rise is due to heat produced by the fuel cell reactions and ohmic heating. As a result, there is an initial sink at the anode entrance region, followed by a gradual rise in temperature, consistent with previous works [32,33].

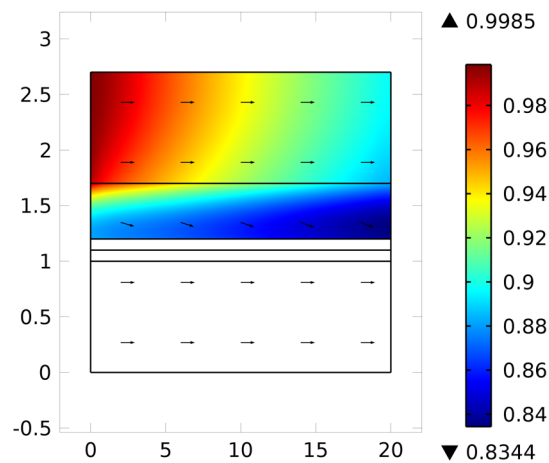


Figure 2. Ammonia Mole Fraction.

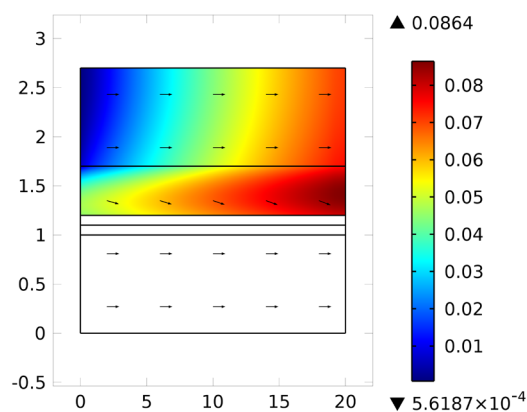


Figure 3. Hydrogen Mole Fraction.

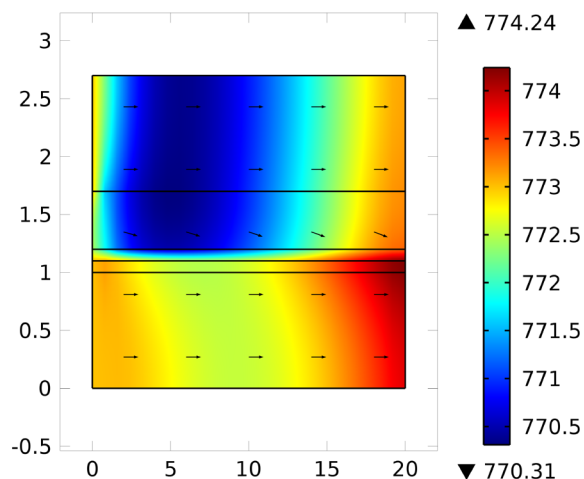


Figure 4. Temperature Distribution (units: K).

## 4 Discussion

The results presented in the previous section are based on an operating cell potential of 0.7 V, a current density of 5000 A/m<sup>2</sup>. It should be noted that in our previous model of a high temperature ammonia-fed SOFC [33], the cell potential was 0.45 V with a current density of 3940 A/m<sup>2</sup>. This means that the present intermediate temperature SOFC produces a power density of 3500 W/m<sup>2</sup>, compared to 1773 W/m<sup>2</sup> for the high temperature SOFC. The intermediate temperature SOFC produces nearly twice as much power as the equivalent high temperature SOFC primarily because of the high conductivity of the proton conducting electrolyte.

Figure 2 showed that the ammonia utilization is only 17% at the temperature used in this work. This is compared to 100% in the previous high temperature model [33]. These results demonstrate that even though the rate of ammonia decomposition decreased with temperature, the fuel cell performance was not compromised at intermediate temperature operation.

The lower rate of ammonia decomposition is attributed to two factors: reduced kinetic rates as well as hydrogen inhibition occurring at the lower temperature. This conversion can be improved by recycling the anode exhaust as shown in our previous work [33], as well as pressurizing the ammonia. However this would also exacerbate the temperature sink.

In high temperature SOFCs, this temperature sink is much more pronounced. In previous models for high temperature ammonia-fed SOFCs, temperature sinks of 67 °C have been reported [32,33], which pose deleterious material problems. In this work, the temperature sink is only 3 °C. This is primarily due to the reduced rate of ammonia decomposition. The results shown in this work suggest that problems of thermal shock can be significantly reduced by operating ammonia-fed SOFCs at intermediate temperatures.

## 5 Conclusion

This work reported the first model of an intermediate temperature ammonia-fed SOFC in the literature. It took into account hydrogen inhibition using Temkin-Pyzhev kinetics. Because of the reduced temperature and the phenomenon of hydrogen inhibition, the rate of ammonia decomposition was lower than high temperature SOFCs, however the fuel cell performance was not compromised. In fact, the results have shown that maintaining a high electrolyte conductivity offsets the effects of reduced ammonia decomposition rates at the lower temperature.

The results have shown that the temperature sink (also known as the “cold spot”) associated with the endothermic ammonia decomposition reaction was significantly mitigated at intermediate temperature operation primarily because of the reduced rate of ammonia decomposition.

In future publications, the author plans to further develop modelling of intermediate temperature SOFCs to include comparisons between Tamaru and Temkin-Pyzhev kinetics at various temperatures, and also to consider a combination of both models at the critical temperature range.

## References

1. C. Zamfirescu and I. Dincer, “Using ammonia as a sustainable fuel,” *J. Power Sources*, vol. 185, pp. 459–465, 2008.
2. J.O. Jensen, A.P. Vestbo, Q. Li and N.J. Bjerrum, “Development of a high pressure microbalance for hydrogen storage materials”, *J. Alloys Compd.* Vol. 446-447, pp. 723–728, 2007.
3. L.M. Zhang, Y. Cong, W.S. Yang and L.W. Lin, “The energy efficiency of onboard hydrogen storage”, *Chinese J. Catalysis*, vol. 28, pp. 749–751, 2007.
4. L. Pelletier, A. McFarlan and N. Maffei, “Ammonia fuel cell using doped barium cerate proton conducting solid electrolytes,”, *J. Power Sources*, vol. 145, pp. 262–265, 2005.
5. N. Maffei, L. Pelletier, J.P. Charland and A. McFarlan, “Direct ammonia fuel cell using barium cerate proton conducting electrolyte”, *J. Power Sources*, vol. 140, pp. 264–267, 2005.
6. Q.L. Ma, R.R. Peng, L.Z. Tian and G.Y. Meng, “Direct utilization of ammonia in intermediate-temperature solid oxide fuel cells”, *Electrochem. Comm.* Vol. 8, pp. 1791–1795, 2006.
7. D. Cheddie, “Ammonia as a hydrogen source for fuel cells: a review,” in: D. Minic, Ed., *Hydrogen Energy – Challenges and Perspectives*, InTech Publishers, 2012, pp. 333-362.
8. R. Lan, J.T.S. Irvine and S. Tao, “Ammonia and related chemicals as potential indirect hydrogen storage materials”, *Int. J. Hydrogen Energy*, vol. 37, pp. 1482 -1494, 2012.
9. T.V. Choudhary, C. Svadinaragana and D.W. Goodman, “Catalytic ammonia decomposition: COx-free hydrogen production for fuel cell applications”, *Catal. Lett.* Vol. 72, pp. 197, 2001.
10. S.F. Yin, Q.H. Zhang, B.Q. Xu, W.X. Zhu, C.F. Ng and C.T. Au, “Investigation on the catalysis of COx-free hydrogen generation from ammonia”, *J. Catal.* Vol. 224, pp. 384, 2004.
11. S.F. Yin, B.Q. Xu, S.J. Wang, C.F. Ng and C.T. Au, “MgO-CNTs (Magnesia-carbon nanotubes) nanocomposites: Novel support of Ru catalysts for the generation of COx free hydrogen from ammonia”, *Catal. Lett.* Vol. 96, pp. 113, 2004.
12. S.J. Wang, S.F. Yin, L. Li, B.Q. Xu, C.F. Ng and C.T. Au, “Investigation on modification of Ru-CNTs catalysts for the generation of COx free hydrogen from ammonia”, *Appl. Catal. B: Env.* Vol. 52, pp. 287, 2004.
13. H.C. Liu, H. Wang, J.H. Shen, Y. Sun and Z.M. Liu, “Preparation, characterization and activities of the nano-sized Ni/SBA-15 catalyst for producing COx-free hydrogen from ammonia”, *App. Catal. A: Gen.* vol. 337, pp. 138–147, 2008.
14. X.K. Li, W.J. Ji, J. Zhao, S.J. Wang and C.T. Au, “Ammonia decomposition over Ru and Ni catalysts supported on fumed SiO<sub>2</sub>, MCM-41, and SBA-15”, *J. Catal.* Vol. 236, pp. 181–189, 2005.
15. J. Zhang, H.Y. Xu, X.L. Jin, Q.J. Ge and W.Z. Li, “Characterizations and activities of the nano-sized Ni/Al<sub>2</sub>O<sub>3</sub> and Ni/La-Al<sub>2</sub>O<sub>3</sub> catalysts for NH<sub>3</sub> decomposition”, *App. Catal. A*, vol. 290, pp. 87–96, 2005.
16. W.Q. Zheng., J. Zhang, Q.J. Ge, H.Y. Xu and W.Z. Li, “Effects of CeO<sub>2</sub> addition on Ni/Al<sub>2</sub>O<sub>3</sub> catalysts for the reaction of ammonia decomposition to hydrogen”, *App. Catal. B: Env.* vol. 80, pp. 98, 2008.
17. C. Plana, S. Armenise, A. Monzón and E. García-Bordejé, “Ni on alumina-coated cordierite monoliths for in situ generation of CO-free H<sub>2</sub> from ammonia”, *J. Catalysis*, vol. 275, pp. 228–235, 2010.
18. Y. Lin, R. Ran, Y. Guo, W. Zhou, R. Cai, J. Wang and Z. Shao, “Proton conducting fuel cells operating on hydrogen, ammonia and hydrazine at intermediate temperatures”, *Int. J. Hyd. En.*, Vol. 35, pp. 2637, 2010.
19. A.S. Chellappa, C.M. Fisher and W.J. Thomson, “Ammonia decomposition kinetics of Ni-Pt/Al<sub>2</sub>O<sub>3</sub> for PEM fuel cell applications”, *App. Catal. A: Gen.* vol. 227, pp. 231–240, 2002.
20. K. Tamaru, “A ‘new’ general mechanism of ammonia synthesis and decomposition on transition metals”, *Acc. Chem. Research*, vol. 21, pp. 88-94, 1988.

21. S.A. Vilekar, I. Fishtik and R. Datta, "The Peculiar Catalytic Sequence of the Ammonia Decomposition Reaction and its Steady-State Kinetics", *Chem. Eng. Sci.* vol. 71, pp. 333-344, 2012.
22. J. Zhang, H. Xu and W. Li, "Kinetic study of NH<sub>3</sub> decomposition over Ni nanoparticles: The role of La promoter, structure sensitivity and compensation effect", *App. Catal. A: Gen.* vol. 296, pp. 257-267, 2005.
23. S.H. Israni, B.K.R. Nair and M.P. Harold, "Hydrogen generation and purification in a composite Pd hollow fiber membrane reactor: experiments and modeling", *Cat. Today* vol. 139, pp. 299-311, 2009.
24. A. Di Carlo, A. Dell'Era and Z. Del Prete, "3D simulation of hydrogen production by ammonia decomposition in a catalytic membrane reactor", *Int. J. Hydrogen Energy*, vol. 36, pp. 11815-11824, 2011.
25. M. Ni, D.Y.C. Leung and M.K.H. Leung, "Thermodynamic analysis of ammonia fed solid oxide fuel cells: Comparison between proton conducting electrolyte and oxygen ion conducting electrolyte", *J. Power Sources*, vol. 183, pp. 682-686, 2008.
26. E. Baniasadi and I. Dincer, "Energy and exergy analyses of a combined ammonia-fed solid oxide fuel cell system for vehicular applications", *Int. J. Hydrogen Energy*, vol. 36 pp. 11128-11136, 2011.
27. S.A. Hajimolana, M.A. Hussain, W.M.A. Wan Daud and M.H. Chakrabarti, "Dynamic modelling and sensitivity analysis of a tubular SOFC fuelled with NH<sub>3</sub> as a possible replacement for H<sub>2</sub>", *Chem. Eng. Res. and Des.*, vol. 90, pp.1871-1882, 2012.
28. M. Ni, D.Y.C. Leung and M.K.H. Leung, "Electrochemical modelling of ammonia-fed solid oxide fuel cells based on proton conducting electrolyte", *J. Power Sources*, vol. 183, pp. 687-692, 2008.
29. M. Ni, D.Y.C. Leung and M.K.H. Leung, "Mathematical modeling of ammonia-fed solid oxide fuel cells with different electrolytes", *Int. J. Hydrogen Energy*, vol. 33, pp. 5765-5772, 2008.
30. M. Ni, D.Y.C. Leung and M.K.H. Leung, "An improved electrochemical model for the NH<sub>3</sub> fed proton conducting solid oxide fuel cells at intermediate temperatures", *J. Power Sources*, vol. 185, pp. 233-240, 2008.
31. F. Ishak, I. Dincer and C. Zamfirescu, "Thermodynamic analysis of ammonia-fed solid oxide fuel cells", *J. Power Sources*, vol. 202, pp. 157-165, 2012.
32. M. Ni, "Thermo-electrochemical modelling of ammonia-fueled solid oxide fuel cells considering ammonia thermal decomposition in the anode", *Int. J. Hydrogen Energy*, vol. 36, pp. 3153-3166, 2011.
33. D. Cheddie, "Modelling of ammonia-fed solid oxide fuel cells," in: A. Mendez-Vilas (Ed.), *Materials and Processes for Energy: Communicating Current Research and Technological Developments*, Formatex Research Center, 2013, pp. 504-511.
34. D. Cheddie, "Modelling the Hydrogen Inhibition Effect on Ammonia Decomposition", *Journal of Energy and Power Engineering*, vol. 8, pp. 662-669, 2014.
35. R. Suranwarangkul, E. Croiset, M.W.Fowler, P.L. Douglas, E. Entchev and M.A. Douglas, "Performance comparison of Fick's, dusty gas and Stefan-Maxwell models to predict concentration overpotentials of a SOFC anode", *J. Power Sources*, vol. 122, pp. 9-18, 2003.

## Nomenclature

**Table 1.** Abbreviations.

Abbreviation	Meaning
SOFC	Solid oxide fuel cell
NO <sub>x</sub>	Nitrogen oxides
YSZ	Yttria-stabilized zirconia
SDC	Samaria-doped ceria

**Table 2.** Symbols.

Symbol	Meaning
$\beta$	Permeability
$\eta$	Overpotential
$\mu$	Dynamic viscosity
$\varphi$	Electrolyte phase potential
$\rho$	Density
$c$	Molar concentration
$c_p$	Specific heat capacity
$D$	Gas pair diffusivity
$F$	Faraday constant
$H$	Enthalpy
$j$	Current density
$j_0$	Exchange current density
$k$	Thermal conductivity
$M$	Molecular mass
$N$	Molar flow rate
$p$	Partial pressure
$r$	Reaction rate
$R$	Universal gas constant
$S$	Source term
$s$	Entropy
$T$	Temperature
$u$	Fluid velocity
$x$	Mole fraction

**Table 3.** Subscripts and superscripts.

Abbreviation	Meaning
$i,j,k$	Chemical species
$a, c$	Anode, cathode
$e$	Electrolyte phase
$act$	Activation
$ref$	Reference
$eff$	Effective
$T$	Thermal